

DKT1, a novel K⁺ channel from carrot, forms functional heteromeric channels with KDC1

Elide Formentin^{a,*}, Serena Varotto^b, Alex Costa^a, Patrick Downey^c, Monica Bregante^d, Alessia Naso^d, Cristiana Picco^d, Franco Gambale^d, Fiorella Lo Schiavo^a

^a*CIRIBI, Centro Interdipartimentale per le Biotecnologie Innovative, Università di Padova, Viale G. Colombo 3, 35131 Padova, Italy*

^b*Dipartimento di Agronomia Ambientale e Produzioni Vegetali, Università di Padova, Agripolis, Viale dell'Università 16, 35020 Legnaro (Padova), Italy*

^c*Schering-Plough Research Institute, San Raffaele Biomedical Science Park, Via Olgettina 58, 20132 Milan, Italy*

^d*Istituto di Biofisica-CNR, Via DeMarini 6, 16149 Genova, Italy*

Received 13 May 2004; revised 21 July 2004; accepted 21 July 2004

Available online 29 July 2004

Edited by Ulf-Ingo Flügge

Abstract We report the isolation and characterisation of DKT1, a new carrot K⁺ channel α -subunit belonging to the Shaker-like family. DKT1 is expressed in many tissues of the adult plant, suggesting that it may play important roles in both nutrition and other important physiological processes. During embryo development, DKT1 is expressed at later phases implying the involvement of K⁺ in embryo maturation. When co-expressed with KDC1 in *Xenopus* oocytes, DKT1 is able to form functional, heteromeric channels, suggesting that possible interactions between these two ion channels in plant tissues may modulate K⁺ uptake.

© 2004 Federation of European Biochemical Societies. Published by Elsevier B.V. All rights reserved.

Keywords: K⁺ channel; Heteromeric channel; Shaker family; *Daucus carota*

1. Introduction

K⁺ is involved in several key cellular functions such as the maintenance of membrane potential, enzyme activation, stomatal movements and tropisms [1–4]. Over the past decade, reverse genetics and electrophysiological studies have revealed the presence of several families of K⁺ channels. Potassium channels of the Shaker family have been isolated from several plant species where they appear to be involved in several steps which are crucial for K⁺ absorption [5].

Based on DNA sequence analysis, and functional characteristics, these channels can be divided into five groups. Groups I, II and IV contain inward rectifier channels, group III weakly inward rectifier channels, while group V consists of outward rectifying channels [6]. In particular, group IV represents inward rectifier channels, such as *Arabidopsis* AtKC1 and carrot KDC1, whose functions in planta have yet to be

determined. KDC1, the first inward potassium channel isolated from carrot [7], is expressed in roots and root hairs and its *Arabidopsis* homologue AtKC1 has been shown to have a very similar expression pattern [8]. In contrast to AtKC1, which is unable to form functional channels in heterologous systems, KDC1 has been functionally expressed in CHO cells where an initial characterisation of the homomeric channel was performed [7]. A more detailed study was conducted in *Xenopus* oocytes where KDC1 does not form functional homomeric channels alone, however, when co-injected with the *Arabidopsis* KAT1 α -subunit, it forms heteromeric channels. KDC1:KAT1 heteromers show current activation which is significantly different from those of the homomeric KAT1 channel, demonstrating the modulator capability of KDC1 on other channels [9,10].

Heteromerization is a widespread mechanism present in both plants and animals that participates in modulation of potassium permeability [11,12]. In *Arabidopsis* plants, AtKC1 forms heteromeric channels with AKT1 in root hairs, where it acts as a regulatory subunit [8]. In fact, while the *akt1* loss-of-function mutants do not express functional inward rectifier channels, the *atkc1* knock-out mutants still express channels showing different properties with respect to wild-type plants. To further investigate the mechanism of action of KDC1 as a modulator subunit, we focused on its possible partners in vivo. To this end, we isolated a cDNA encoding a novel Shaker-like inward rectifier potassium channel from carrot roots and determined its expression pattern, which was found to partly overlap that of KDC1. Using co-expression techniques in *Xenopus* oocytes, we demonstrate that the two proteins can indeed form functional heteromeric potassium channels.

2. Materials and methods

2.1. Plant materials

Seeds of *Daucus carota* (L.), cv. S. Valery, were sterilized and incubated in Petri dishes, with Gamborg's B5 basal medium (Sigma, Italy) [13] and allowed to germinate in the dark in a growth chamber at 24 °C. Shoot apex and cotyledons were collected 5 days after germination. Leaves, stems and roots were collected 3 weeks after transplantation of germinated seeds in plastic boxes containing Gamborg's B5 medium with 0.5% phytoagar (Micropoli, Italy).

* Corresponding author. Fax: +39-49-827-6159.

E-mail address: elide@mail.cribi.unipd.it (E. Formentin).

Abbreviations: KDC1, K⁺ *Daucus carota* 1; RACE, rapid amplification of cDNA ends; RT-PCR, reverse transcriptase-polymerase chain reaction; SAM, shoot apical meristem; S.D., standard deviation; S.E., standard error

In order to initiate embryogenesis, seven-day old carrot cell cultures were filtered to standardize clump size, and resuspended at low density in basal medium. Embryos of each stage were isolated from these differentiating cultures yielding mixed populations of different embryonic stages as previously described [14].

2.2. RNA extraction and *DKT1* full-length cDNA isolation

10–100 mg of frozen material from carrot was crushed to powder in liquid nitrogen and used for each preparation. Total RNA extraction was performed using the TriZol reagent (Gibco BRL, Germany). After DNaseI treatment (Ambion Ltd, UK), first strand cDNA was synthesized starting from 5 µg of total RNA using the PowerScript™ Reverse Transcriptase (Clontech, USA) and diluted 1:5.

DKT1 partial cDNA was first isolated by PCR using degenerate primers designed against Shaker-like potassium channels conserved regions. The full-length cDNA was obtained by 5' and 3' RACE performed on root total RNA following the manufacturer's instructions (SMART RACE cDNA Amplification Kit, Clontech, USA). This cDNA was cloned into vectors and completely sequenced in both strands.

2.3. Relative-quantitative RT-PCR

Relative-quantitative RT-PCR was carried out with 5 µl of first-strand cDNA, using the 18S rRNA as an internal standard (QuantumRNA 18S Internal Standards Kit, Ambion Ltd, UK). The 18S primers:competimers ratio was established as 1:9.

The *DKT1* amplicon (500 bp) was obtained using the following forward primer 5'-TTCAACTGCCCGAGGAAAAACAC-3' and reverse primer 5'-GAGTTCGGCGCAAATTGAAAC-3'. The cycling parameters were as follows: 20 s at 94 °C, 1 min at 68 °C. The number of cycles (27) was determined as described in the QuantumRNA protocol. Densitometric analysis of ethidium bromide stained agarose gels (0.5 µg/ml) was performed using Quantity One software (Bio-Rad). The relative abundance of the transcript within the samples was calculated as the ratio of the intensities of the *DKT1* amplicon relative to the 18S rRNA amplicon.

2.4. Sequence analysis

The protein coding region in the *DKT1* cDNA sequence was determined using the Translate tool of the Swiss Institute of Bioinformatics (SIB) (www.expasy.ch). Phylogenetic and molecular evolutionary analyses were conducted using MEGA version 2.1 [15] on the basis of the alignment obtained using DAMBE [16]. The sequences were from GenBank database and the accession numbers were the following: KAT1 (NP_199436); KAT2 (NP_193563); SKOR (NP_186934); AtKC1 (CAB79982); AKT2 (NP_567651); AKT5 (NP_194976); SPIK (NP_180131); AKT1 (NP_180233); GORK (NP_198566); PTK2 (CAC0548); PTORK (CAC05488); KPT1 (CAC87141); SIRK (AAL24466); VvSOR (CAD35400); MKTIP (AAF81249); SKT1 (T07651); KST1 (S55349); SKT2 (CAA70870); SPICK1 (AAD16278); SPICK2 (AAD39492); SPORK1 (CAC10514); LKT1 (CAA65254); NpKT1 (BAA84085); EcKT1-1 (AAL25648); EcKT1-2 (AAL25649); VKC1 (T12177); KZM1 (CAD18901); KZM2 (CAD90161); ZMK1 (CAA68912); ZMK2 (CAB54856); ZMK2.1 (AAR21352); TaAKT1 (AAF36832); OsAKT1 (BAC05546); OsK3 (BAB90143); OsK4 (BAB68056); OsK5 (BAA96150); KDC1 (CAB62555); *DKT1* (AJ697979). Sequence similarity searches were performed using the Blast algorithm [17] at NCBI (www.ncbi.nlm.nih.gov). Pattern and profile searches were conducted by mean of Pfam at Sanger Institute (www.sanger.ac.uk). Secondary structure prediction was performed by using PSIPRED [18] (bioinf.cs.ucl.ac.uk/psipred/).

2.5. In situ hybridisation

Plant materials were fixed in 4% paraformaldehyde, 0.2% glutaraldehyde in 0.1 M phosphate buffer (pH 7.2) for 16 h at 4 °C and embedded in Paraplast Plus (Sigma–Aldrich, Italy). Sections (10 µm) were cut using a microtome (RM 2135 Leica, Germany) and collected in xylene-coated slides. Slides were deparaffinized, treated with 5 µg/ml proteinase K and hybridised with sense and antisense riboprobes in 50% formamide at 45 °C overnight. A 500 bp 3' specific cDNA fragment of *DKT1* was amplified by PCR, using the primers listed below, cloned in pCRII-TOPO vector (Invitrogen, UK) and transcribed in vitro to obtain DIG-UTP (Roche, Germany) labelled RNA sense and antisense probes using T7 and Sp6 polymerases. After hybridisation the slides were extensively washed in 2X SSC at 45 °C and treated with

20 µg/ml RNaseA (Roche, Germany). DIG detection and signal visualization were carried out using NBT and BCIP (Roche) following the manufacturer's instructions. Images were acquired using a Leica DC 300F camera.

2.6. Expression in *Xenopus laevis* oocytes and electrophysiology

Injection of RNA in oocytes. *Xenopus laevis* oocytes were isolated [19] and injected with *DKT1* and *KDC1* mRNAs (0.24–5 µg/µl) using a Drummond "Nanoject" microinjector (50 nl/oocyte). RNA concentration was quantified by absorbance spectroscopy. All the experiments presented were performed using a single preparation of the two RNAs (*KDC1* and *DKT1*), although similar results were obtained using other batches. Current recordings were made 2–5 days after injection. In the case of co-expression, *KDC1* and *DKT1* were co-injected at 1:1 molar ratio.

Voltage-clamp recordings. Whole cell K⁺ currents were measured with a two microelectrode home-made voltage-clamp amplifier [10], using 0.2–0.4 Mohm pipettes filled with 3 M KCl. Unless otherwise indicated the following bath standard solution was used (in mM): 100 KCl, 2 MgCl₂, 1 CaCl₂, 10 MES/TRIS (pH 5.6). Each data point represents the mean ± S.E. obtained from at least three different experiments. Holding potential was 0 mV and currents were typically filtered with a cut-off frequency of 3 kHz.

3. Results

3.1. Cloning of *DKT1* cDNA from carrot roots

In order to isolate new Shaker-like potassium channels, RT-PCR experiments were performed using degenerate primers designed on the highly conserved pore region. Starting with root RNA, we isolated a full-length cDNA of 2827 bp which contains an open reading frame of 2622 bp encoding a predicted protein of 873 amino acids (MW = 99 kDa; pI 7.06). Sequence similarity searches revealed that this putative protein has a strong identity (82%) to *Arabidopsis* Shaker-like potassium channel AKT1 [20] and to potassium channels of the AKT1 family cloned from other plant species, such as tomato LKT1 (85%) [21]. The high degree of homology between the cloned protein and AKT1 allowed its attribution to the AKT1 group of Shaker-like potassium channels [6] as shown in Fig. 1. We named this second carrot potassium channel gene *DKT1*, according to its homology with AKT1.

The hydrophobicity profile and the PSIPRED output for this putative protein revealed the presence of six transmembrane elements (Fig. 2), which is a typical membrane topology for potassium channels belonging to the Shaker-like family. Other domains were predicted by using Pfam, namely a cyclic nucleotide binding domain (cNBD) between amino acids 390 and 482, six ankyrin tandem repeats (ANK1–ANK6) between residues 520 and 721, a hydrophilic C-terminal domain (K_{HA}), and the TxxTxGYGD consensus sequence for K⁺ selectivity [22] in the pore region (Fig. 2).

3.2. Expression pattern profile of the *DKT1* gene

DKT1 is a single copy gene in the carrot genome (data not shown), and its expression pattern was investigated in different mature plant tissues and stages of embryo development by RT-PCR and in situ hybridization.

Analysis in mature plants. Relative-quantitative RT-PCR was performed on total RNA extracted from several plant tissues. These experiments detected the highest levels of the *DKT1* transcript in leaves and in shoot apex but expression was also detected in roots, cotyledons and stems (Fig. 3). In order to determine the cellular localisation of the *DKT1* transcript in plant roots, in situ hybridisation experiments were

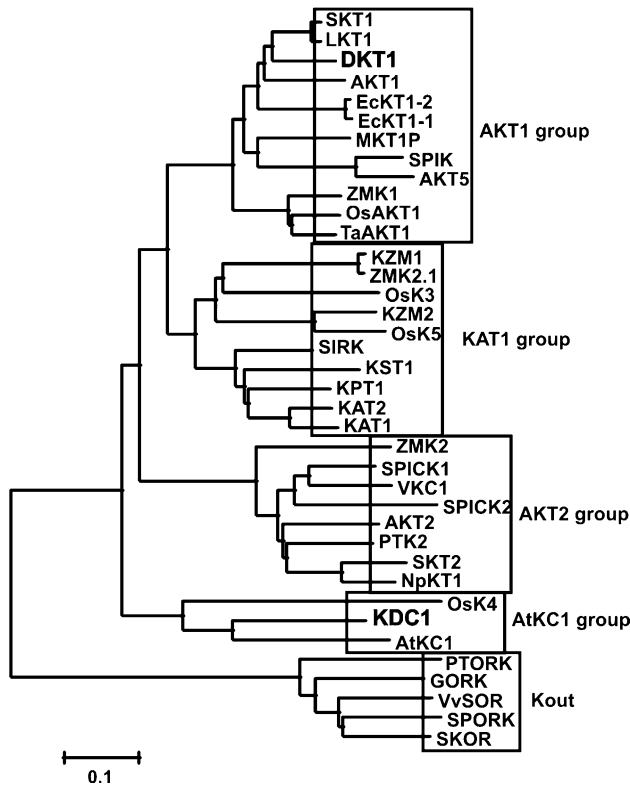


Fig. 1. Phylogenetic tree showing that DKT1 belongs to the AKT1 group of plant Shaker-like potassium channels.

performed on seedling root sections. In plantlet roots, *DKT1* showed low and constitutive expression. Comparing root sections hybridised with the sense (Fig. 4A) and antisense (Figs. 4B and C) riboprobes after three days incubation in the staining solution, the signal was detectable in the epidermis, cortex, endodermis, pericycle and vascular cylinder. A weak hybridisation signal was also present in root hairs (Fig. 4C). In both young and mature leaves *DKT1* was expressed mainly in the lower and upper epidermis and around the veins (Fig. 4E).

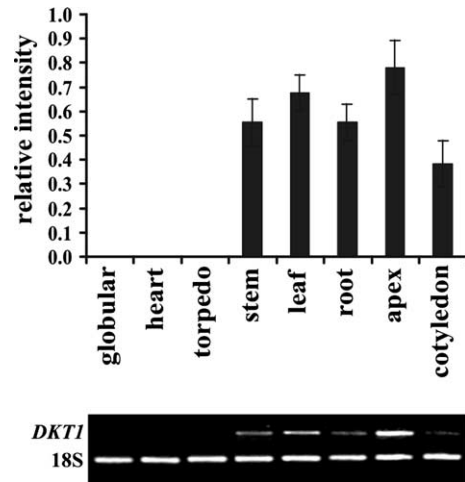


Fig. 3. Expression pattern analysis of *DKT1* in different carrot tissues by relative-quantitative RT-PCR. In the upper panel the relative abundance of *DKT1* transcript is shown. Data are reported as mean values \pm S.D.; $n = 3$. In the lower panel, an ethidium bromide stained gel of the RT-PCR products showing the typical pattern obtained for this transcript is presented.

A hybridization signal was also detected in leaf trichomes (Fig. 4F) and stomatal cells (Fig. 4G). Five days after germination, carrot seedlings were embedded in order to obtain sections through the SAM. The expression of *DKT1* in SAM was localised in the L1 and L2 layers, which will generate leaf epidermis and mesophyll, in leaf primordia and in developing leaves (Fig. 4H).

Analysis during embryo development. As carrot is a model system for cell cultures and somatic embryogenesis, we analysed the pattern of expression of *DKT1* during embryogenesis. The transcript was not found in any of the purified somatic embryo forms (globular, heart, torpedo) as analysed by relative-quantitative RT-PCR (Fig. 3). This is in agreement with in situ hybridization experiments carried out in carrot ovary during seed maturation. During zygotic embryogenesis the hybridisation signal was not detectable in early phases of

```

MFKVPVICGTELEREIELSRDGSYSLTTGILPSPGLGARSNRRVQLRNFIIISPYDRRYRFWETFLVILVIYTAVVSPFELGFLHKARPPLS 90
                                                                                               S1
VLDNVVNGFFAIDIVLTFVAYLDRNTYLLIDDRKLIWKYTSTWLAFDVISTIPSELALKISPSPLRITYGLFNMLRLWRLRRVSSLFAR 180
S2                                                                                               S3                                                                                               S4
LEKDRNFNFYFWRCAKLIQVTLFAVHSSACFYLLAADYHDPKSTWIGASITDFKNQSLWIRYVTSIYWSITLTTVGYGDLHAQNTGEM 270
S5                                                                                               H5
IYDIFYMLFNLGLTAYLIGNMNTNLVHGTSKTRQFRDITQAASSFAHRNRLPVRLQDQMLAHLCLKFRDSEGLQQQETLDTLPKAISS 360
S6
ISHFLFYTLVDKVIYFRGVSNDLLFLQVSEMKAEYFPPKEDVILQNEAPTDFYILVTGAVDLVVLKNGVEQVVEAKTGDLCEIGVLCY 450
                                                                                               cNBD
RPQLFTARTKRLSOLLRLNRTTFNIIQANVGDGTIIMNNLLQHLIEKDPMMEGVLETEHMLARGRMDLPLSLCFATLRGDDQLLNQL 540
                                                                                               ANK1
LKRGLDPNESDNNRNTALHIAASKGNENCVLLLLLDYGADPNRSRDEGNVPLWEAMLSNHEQVVKVVLADNGAVISSGDTGYFACIAAEQNN 630
                                                                                               ANK2                                                                                               ANK3
LDLLKEIVHRGGDVTTPKSNGATALHVAVCEGNVDIVKFLLDQGCYADKADHWGTPRNLAEQQGHEDIKLLFQSPKPERTQSADVQLPE 720
ANK4                                                                                               ANK5                                                                                               ANK6
EKHGVRFGLGRHSEPTIRPFSDHRNGEGESLGRARRRRGNFNHNSLFGIMSSATGEENDLLSVNQNRSAALNVAHYHTARTTVSACPQKGDV 810
TGKLVLLPQSFQQLLEICMKKYRFVPTRVLIKDGAEIDEINLVRDGDHLVFGDLTVNGGHMR 873
                                                                                               KHA
    
```

Fig. 2. Predicted amino acid sequence of *DKT1*. The predicted six transmembrane domains (S1–S6), the pore forming region (H5) leading the K^+ selectivity consensus sequence (boxed), the cNBD, the six ankyrin repeats (ANK1–6) and the C-terminal K_{HA} domain are underlined.

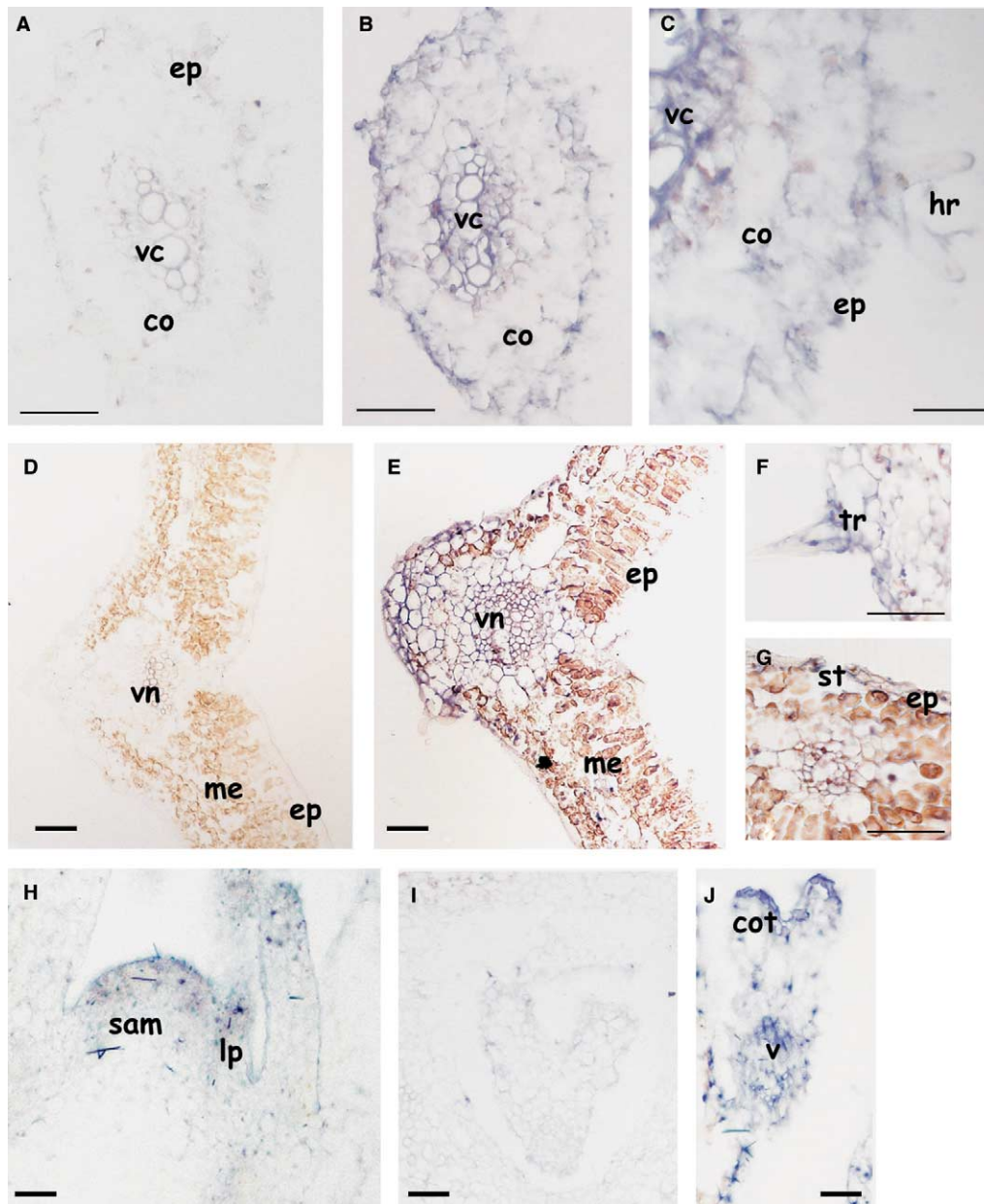


Fig. 4. In situ localisation of *DKT1* in plants. The blue staining represents the hybridisation signal. (A)–(C) Root cross sections of carrot seedling. In (A) the section was hybridised with a *DKT1* sense transcript and no signal is detectable. In (B) the hybridisation was carried out using the antisense *DKT1* riboprobe. (C) Higher magnification of (B). (D)–(G) Leaf cross sections. In (D) the section was hybridised with the *DKT1* sense riboprobe and no signal was detected. In (E) the leaf section was hybridised with the *DKT1* antisense transcript. (F) Higher magnification of (E) showing a leaf trichome. (G) Higher magnification of (E) showing a stomata. (H) Longitudinal section of carrot shoot apex hybridised with the *DKT1* antisense riboprobe. (I)–(J) Cross sections through a carrot ovary hybridised with *DKT1* antisense riboprobe. (I) Zygotic embryo at the heart stage. (J) Embryo at the torpedo stage. co: cortex; cot: cotyledon; ep: epidermis; hr: root hair; lp: leaf primordium; me: mesophyll; sam: shoot apical meristem; st: stomata; tr: trichome; v: vasculature; vc: vascular cylinder; vn: veins. Bars 100 µm, in (A), (B), (D), (E), (H), (I), and (J), and 50 µm, in (F) and (G).

embryogenesis at either the globular or heart stage (Fig. 4I), but a signal was clearly visible in embryo cotyledons and around the vasculature at the torpedo stage (Fig. 4J). It is probable that the signal was not visible in somatic embryos because they show limited cotyledon development as compared to zygotic embryos [23].

3.3. Functional characterization in *Xenopus* oocytes: *DKT1* co-assembles with *KDC1*

In an attempt to analyse the functional properties of *DKT1* in heterologous systems, we found that *DKT1* is unable to

form functional channels by itself when injected in *Xenopus* oocytes. Indeed, oocytes injected with *DKT1* alone displayed currents undistinguishable from controls (Fig. 5C). Moreover, functional expression of *DKT1* could not be observed in HEK293, N2A or CHO cells, mammalian cell lines typically used as heterologous expression systems for ion channels.

The results presented on *DKT1* localization together with the whole mount and in situ hybridisation experiments reported for *KDC1*, the first potassium channel isolated from carrot [7,24], demonstrate that the channels are co-localised in many plant tissues, in roots (endodermis, epidermis and hairs),

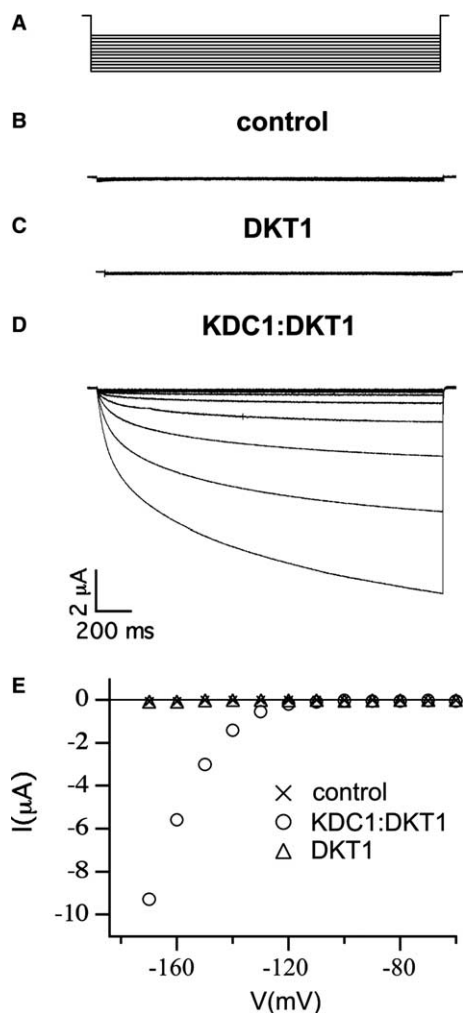


Fig. 5. Functional co-expression of KDC1 and DKT1 in oocytes. (A) Voltage steps (from -60 to -180 mV) were applied in 10 mV increments. (B) Ionic currents in uninjected (control) oocytes. (C) currents in oocytes injected with DKT1 and (D) in oocytes co-injected with KDC1:DKT1. (E) Current voltage characteristics of the family of currents shown in (B, C, D) obtained by plotting the mean value of the current during the last 50 ms in each record as a function of the applied membrane potential.

SAM and embryo cotyledons (summed up in Table 1), therefore suggesting a possible interaction between the two channels. It has been widely demonstrated that plant K^+ channels can co-assemble [8–11,25], and we have previously shown that KDC1 can act as a modulator subunit when co-expressed with KAT1 [9,10], we thus wanted to see if KDC1 can form functional heteromeric channels with DKT1. Interestingly, we obtained exceptionally robust and stable negative inwardly-rectifying ionic currents in almost all oocytes which were co-injected with KDC1 and DKT1. Fig. 5D shows typical KDC1:DKT1 currents, which activate in a time dependent manner at membrane potentials more negative than -120 mV (Fig. 5E). This suggests the formation of heteromultimeric channels between KDC1 and DKT1 subunits. In line with the results obtained with KDC1, which forms heteromeric potassium channels with KAT1 [9], the ability of DKT1 to form heteromultimeric channels with KAT1 was also verified by the co-expression in *Xenopus* oocytes. The DKT1:KAT1 channel

Table 1
Overlapping expression pattern between *KDC1* and *DKT1*

Tissue or organ		<i>KDC1</i>	<i>DKT1</i>
Somatic embryo (protoderm)	Globular stage	+	-
	Heart stage	+	-
	Torpedo stage	+	-
Zygotic embryo	Torpedo stage (cotyledon)	+	+
Plantlet	Root epidermis (root hair)	+	+
	Root endodermis	+	+
	Root cortex	-	+
	Cotyledon	-	+
	Stem	-	+
	SAM	+	+
Leaf	-	+	

List of plant tissues and embryonic stages where the expression pattern of *KDC1* [24] and *DKT1* was analysed by whole mount or in situ hybridisation. The '+' and '-' symbols indicate the presence or the absence of the transcript.

displayed large inward rectifying currents with modified characteristics with respect to homomeric KAT1 (data not shown).

The heteromeric KDC1:DKT1 channels were potassium-selective. Indeed, KDC1:DKT1 current amplitude depends on K^+ concentrations, as demonstrated by experiments where external media contained different concentrations of KCl and NaCl to a total salt concentration of 100 mM (Fig. 6A). Upon variation of the K^+ concentration in the bath, the reversal potentials determined by tail current experiments shifted by (55 ± 3) mV for a 10-fold change in the K^+ gradient, indicating the high selectivity of the channel for potassium over sodium. Fig. 6B shows an example of tail currents recorded at an external potassium concentration equal to 30 mM. In Fig. 6C the reversal potentials are plotted against the potassium activity. Moreover, the inward rectifying KDC1:DKT1 channel was blocked by millimolar concentrations of external caesium as shown in Fig. 6D, where a typical decrease of the current following the addition of CsCl in the bath solution is shown.

4. Discussion

This paper describes the isolation of a new transcript encoding a K^+ inward rectifier channel from carrot, namely DKT1. This channel belongs to the AKT1 group of plant Shaker channels [6], showing high sequence homology and structural similarities with the other AKT1-like channels (Figs. 1 and 2).

The analysis of the gene expression (Figs. 3 and 4) reveals similar pattern to that of *AKT1*: both genes are expressed in roots and root hairs [26,27] where they may have a nutritional role [28]. In leaves, *DKT1* shows a wider expression profile than its *Arabidopsis* homologue [26,29], and its presence in guard cells suggests an involvement in stomatal movements. The temporal expression of *DKT1* in zygotic cotyledons, suggests a role of DKT1 in cotyledon expansion during late phases of embryo maturation. Concerning hormonal regulation, neither *AKT1* [30] nor *DKT1* are regulated by auxin. In our system, young seedlings and mature plants were isolated and incubated with auxin and the expression pattern of the gene was analysed by semi-quantitative RT-PCR in different tissues (root, stem, leaf, shoot apex and cotyledons) (data not

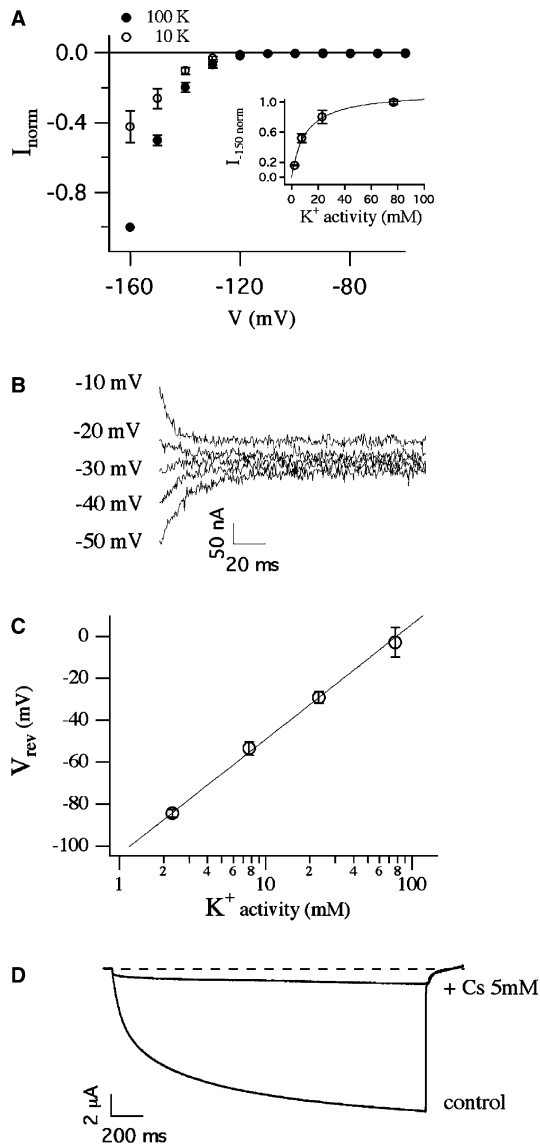


Fig. 6. The heteromeric KDC1:DKT1 channel is potassium-selective. (A) Average normalized current–voltage characteristics are shown for two different potassium concentrations. Currents were elicited by 2 s hyperpolarizing pulses from -60 to -160 mV in -10 mV steps. *Inset*: normalized current at -150 mV as a function of potassium activities 2.3, 7.7, 23.1, 77 mM. (B) Representative tail currents elicited by a tail pulse from -10 to -50 mV (at -10 mV decrements) following a conditioning prepulse to -150 mV. (C) Reversal potential V_{rev} of the currents carried by the heteromeric channels upon variation of the external K^+ activity. The continuous line represents the best fit of experimental data points, revealing a shift in V_{rev} of 55 mV per 10-fold change in the K^+ gradient. (D) KDC1:DKT1 current was reversibly inhibited by 5 mM Cs^+ . Voltage steps to -150 mV.

shown). In contrast, in the monocotyledonous *Zea mays*, the AKT1-like channel ZMK1 is under the control of auxin, especially in the coleoptile tissue [31,32], suggesting a different auxin response in mono- and dicotyledonous plant species.

The electrophysiological experiments conducted in *Xenopus* oocytes demonstrated that DKT1, like KDC1, injected individually does not form a functional channel. In contrast, we demonstrated the formation of heteromeric KDC1:DKT1 channels that are able to mediate robust and stable inward

currents that activated at hyperpolarizing membrane potentials. These currents are mediated by typical potassium selective channels, as demonstrated by the shift of the reversal potential with K^+ concentration and their block by external caesium (Figs. 5 and 6). These results together with ones reported by Duby et al. [33] might open the possibility for the identification and characterisation of new mechanisms controlling channel targeting to the cell membrane. In addition, KDC1 is an excellent model subunit owing to its peculiar histidine composition and “tolerance” to metals [9,10] while more studies are needed to identify a more precise functional fingerprinting of DKT1.

In conclusion, we report, for the first time, evidence that α -subunits belonging to the same species and present in the same tissues (see Table 1) can cooperate to form functional heteromeric plant K^+ channels. We suggest that a different behaviour in K^+ absorption could be determined by a differential expression of these two (and possibly other) subunits. It seems reasonable that plants may have adopted this modulator strategy to respond to different environmental conditions and external stresses. However, we cannot exclude that in tissues where KDC1 is not present (e.g. guard cells, see Table 1), DKT1 may form homomeric channels or interact with other as of yet unidentified subunits. The study of DKT1 in transgenic plants and a complete characterisation of the heteromultimeric KDC1:DKT1 channel should be forthcoming.

Acknowledgements: We thank Dr. Armando Carpaneto, Dr. Ildikò Szabò and Prof. Mario Terzi for a critical reading of the manuscript. This research was supported by the Ministero dell’Istruzione e della Ricerca, Fondi per gli Investimenti della Ricerca di Base, Project N-RBAU0183A9 and by a contribution from Consorzio Interuniversitario Biotecnologie (CIB) to FLS.

References

- [1] Brüggemann, L., Dietrich, P., Becker, D., Dreyer, I., Palme, K. and Hedrich, R. (1999) Proc. Natl. Acad. Sci. USA 96, 3298–3302.
- [2] Clarkson, D.T. and Hanson, J.B. (1980) Annu. Rev. Plant Physiol. 31, 239–298.
- [3] Schroeder, J.I. and Hedrich, R. (1989) Trends Biochem. Sci. USA 87, 9305–9309.
- [4] Mouline, K., Véry, A.A., Gaymard, F., Boucherez, J., Pilot, G., Devic, M., Bouchez, D., Thibaud, J.B. and Sentenac, H. (2002) Genes Dev. 16, 339–350.
- [5] Véry, A.A. and Sentenac, H. (2003) Annu. Rev. Plant Physiol. Plant Mol. Biol. 54, 575–603.
- [6] Pilot, G., Pratelli, R., Gaymard, F., Meyer, Y. and Sentenac, H. (2003) J. Mol. Evol. 56, 418–434.
- [7] Downey, P., Szabò, I., Ivashikina, N., Negro, A., Guzzo, F., Ache, P., Hedrich, R., Terzi, M. and Lo Schiavo, F. (2000) J. Biol. Chem. 275, 39420–39426.
- [8] Reintanz, B., Szyroki, A., Ivashikina, N., Ache, P., Godde, M., Becker, D., Palme, K. and Hedrich, R. (2002) Proc. Natl. Acad. Sci. USA 99, 4079–4084.
- [9] Paganetto, A., Bregante, M., Downey, P., Lo Schiavo, F., Hoth, S., Hedrich, R. and Gambale, F. (2001) J. Bioenerg. Biomembr. 33, 63–71.
- [10] Picco, C., Bregante, M., Naso, A., Gavazzo, P., Costa, A., Formentin, E., Downey, P., Lo Schiavo, F. and Gambale, F. (2004) Biophys. J. 86, 224–234.
- [11] Dreyer, I., Antunes, S., Toshinori, H., Müller-Röber, B., Palme, K., Pongs, O., Reintanz, B. and Hedrich, R. (1997) Biophys. J. 72, 2143–2150.
- [12] Finn, J.T., Krautwurst, D., Schroeder, J.E., Chen, T.Y., Reed, R.R. and Yau, K.W. (1998) Biophys. J. 74, 1333–1345.
- [13] Gamborg, O.L., Miller, R.A. and Ojima, K. (1968) Exp. Cell Res. 50, 151–158.

- [14] Giuliano, G., Rosellini, D. and Terzi, M. (1983) *Plant Cell. Rep.* 2, 216–218.
- [15] Kumar, S., Tamura, K., Jakobsen, I.B. and Nei, M. (2001) *Bioinformatics* 17, 1244–1245.
- [16] Xia, X. and Xie, Z. (2001) *J. Heredity* 92, 371–373.
- [17] Altschul, S.F., Gish, W., Miller, W., Myers, E.W. and Lipman, D.J. (1990) *J. Mol. Biol.* 215, 403–410.
- [18] Jones, D.T. (1999) *J. Mol. Biol.* 292, 195–202.
- [19] Hedrich, R., Moran, O., Conti, F., Bush, H., Becker, D., Gambale, F., Dreyer, I., Kuch, A., Neuwinger, K. and Palme, K. (1995) *Eur. Biophys. J.* 24, 107–115.
- [20] Sentenac, H., Bonneaud, N., Minet, M., Lacroute, F., Salmon, J.M., Gaymard, F. and Grignon, C. (1992) *Science* 256, 663–665.
- [21] Hartje, S., Zimmermann, S., Klonus, D. and Müller-Röber, B. (2000) *Planta* 210, 723–731.
- [22] Schachtman, D.P. (2000) *Biochem. Biophys. Acta* 1465, 127–139.
- [23] Steeves, T.A. and Sussex, I.M. (1989) *Patterns in plant development*. Cambridge University Press, Cambridge, MA.
- [24] Costa, A., Carpaneto, A., Varotto, S., Formentin, E., Marin, O., Barizza, E., Terzi, M., Gambale, F., and Lo Schiavo, F. (in press) *Plant Mol. Biol.* Available from: www.kluwer.com/issn/0167-4412.
- [25] Pilot, G., Gaymard, F., Mouline, K., Chérel, I. and Sentenac, H. (2003) *Plant Mol. Biol.* 51, 773–787.
- [26] Lagarde, D., Basset, M., Lepetit, M., Conejero, G., Gaymard, F., Astruc, S. and Grignon, C. (1996) *Plant J.* 9, 195–203.
- [27] Ivashikina, N., Becker, D., Ache, P., Meyerhoff, O., Felle, H.H. and Hedrich, R. (2001) *FEBS Lett.* 508, 463–469.
- [28] Dennison, K.L., Robertson, W.R., Lewis, B.D., Hirsch, R.E., Sussman, M.R. and Spalding, E.P. (2001) *Plant Physiol.* 127, 1012–1019.
- [29] Szyroki, A., Ivashikina, N., Dietrich, P., Roelfsema, M.R.G., Ache, P., Reintanz, B., Deeken, R., Godde, M., Felle, H., Steinmeyer, R., Palme, K. and Hedrich, R. (2001) *Proc. Natl. Acad. Sci. USA* 98, 2917–2921.
- [30] Philippar, K., Ivashikina, N., Ache, P., Christian, M., Lüthen, H., Palme, K. and Hedrich, R. (2004) *Plant J.* 37, 815–827.
- [31] Philippar, K., Fuchs, I., Lüthen, H., Hoth, S., Bauer, C.S., Haga, K., Thiel, G., Ljung, K., Sandberg, G., Bottger, M., Becker, D. and Hedrich, R. (1999) *Proc. Natl. Acad. Sci. USA* 96, 12186–12191.
- [32] Fuchs, I., Philippar, K., Ljung, K., Sandberg, G. and Hedrich, R. (2003) *Proc. Natl. Acad. Sci. USA* 100, 11795–11800.
- [33] Duby, G., Hosy, E., Broekgaarden, C., Costa, A., Vavasseur, A., Mouline, K., Thibaud, J.B., and Sentenac, H. (2004) In: 13th International Workshop on Plant Membrane Biology, Montpellier, July 6–10. Oral session T4-3, p. 34.